Thermal Chemistry of Iodomethane on Ni(110). 1. Clean and Hydrogen-Predosed Surfaces

Hansheng Guo and Francisco Zaera*

Department of Chemistry, University of California, Riverside, California 92521

Received: July 6, 2004; In Final Form: July 30, 2004

The thermal chemistry of iodomethane on Ni(110) single-crystal surfaces was studied by temperature-programmed desorption (TPD) and X-ray photoelectron spectroscopy. The activation of the C−I bond occurs by 150 K, and produces methyl surface moieties. Hydrogen desorption is always seen, in one peak at 350 K at low coverages and in additional lower temperature regimes above a 1.0 langmuir CH_3I exposure. Methane is also produced, in an initial peak at 274 K for 1.0 langmuir, and mainly in a second feature at 238 K on saturated surfaces. Additional experiments with CD_3I and with coadsorbed hydrogen or deuterium indicate that the hydrogenation step of methyl to methane is controlled by the population of surface hydrogen, which originates either from decomposition of some of the methyl intermediates and/or from preadsorption. Interestingly, and in contrast to what is observed on Ni(100) or Ni(111) surfaces, some production of heavier hydrocarbons is seen on this Ni(110) surface at about 188 K at high CH_3I coverages. A mechanism is proposed where an initial dehydrogenation of some of the adsorbed methyl to methylene surface species is followed by a rate-limiting methylene migratory insertion into a metal−alkyl (methyl) bond to yield a heavier alkyl (ethyl) intermediate. Facile subsequent β-hydride and reductive eliminations (the latter with surface hydrogen) account for the formation of the alkenes and alkanes seen in the TPD experiments, respectively.

1. Introduction

Methyl (CH_3), methylene (CH_2), and methylidyne (CH) are crucial intermediates in many hydrocarbon conversion processes of industrial interest, including Fischer−Tropsch,[1,2] methanation,[3] and natural gas[4] conversions. As the reactivity of those C_1 adsorbates varies with the properties of the catalyst, it is possible to tune the selectivity to favor a given process. However, to be able to design catalysts with optimized selectivity from first principles, a fundamental understanding of the mechanistic parameters that control the reactivity of different catalytic surfaces is required.[5] Studies of adsorption and reactivity of methyl and methylene species on single crystals afford the opportunity to identify and examine the surface chemistry of C_1 hydrocarbon fragments at a molecular level.[6,7]

Extensive surface-science work has been carried out on the characterization of methyl groups on transition-metal surfaces.[8−12] Typically, total dehydrogenation to H_2 and surface carbon and/or hydrogenation to methane is observed. On coinage metals, however, coupling to ethane is also feasible.[13,14] Perhaps the most interesting case is that of copper, where chain propagation to heavier hydrocarbons has been observed.[15−17] A dependence of the methyl conversion on the structure of the surface has been identified on that metal, with the smooth Cu(100) promoting the rate of carbon chain growth at about 2 orders of magnitude faster rate than the more open Cu(110).[18] On nickel, our previous work has proven that the thermal conversion of methyl on (100)[19−22] and (111)[23] surfaces leads to the exclusive desorption of hydrogen and methane, as with most other transition metals. The thermal chemistry of CH_3I on Ni(110) has also been predicted theoretically to be similar to that on Ni(100).[24] On the other hand, the chemistry of methylene moieties on Ni(110)[25] is much richer than that reported previously on the smoother (100) plane.[21,26] This prompted us to test the chemistry of methyl species on the (110) surface.

Here we report on the thermal chemistry of CH_3I on clean and hydrogen (deuterium)-predosed Ni(110) single-crystal surfaces. As in other work from our laboratory, here we have relied on the use of a halohydrocarbon, iodomethane, as the precursor for the production of an important surface intermediate in catalysis, methyl groups.[27,28] Indeed, this approach has been shown by us[27,29,30] and others[9,11,12,31,32] to be quite universal. In particular, it has been established that the C−I bond in adsorbed iodohydrocarbons dissociates around 150 K,[33,34] and that the co-deposited iodine atoms do not severely interfere in the subsequent surface chemistry of the hydrocarbon species.[9,35−37] As with the other nickel surfaces, the chemistry of methyl species prepared by iodomethane activation on Ni(110) was found to be dominated by hydrogen and methane formation. However, the production of significant amounts of heavier hydrocarbons was detected as well. In this paper we provide the details of this chemistry, together with evidence for a chain growth mechanism based on methylene migratory insertion steps similar to those seen on copper single crystals[17] and proposed for iron-based Fischer−Tropsch processes.[1]

2. Experimental Section

The experiments were conducted in an ultra-high-vacuum (UHV) system with a base pressure of 1×10^{-10} Torr.[38,39] The system is equipped with a UTI mass quadruple for temperature-programmed desorption (TPD), and a dual-anode X-ray source and a concentric hemispherical analyzer (VG 100AX) for X-ray photoelectron spectroscopy (XPS).

A polished Ni(110) single-crystal sample, a disk 10 mm in diameter and 1 mm in thickness, was used. Two 0.5 mm Ta wires were spot-welded to the edge of the crystal and fixed on the ends of two copper vacuum feedthroughs, the other ends of

* To whom correspondence should be addressed. E-mail: zaera@ucr.edu.

10.1021/jp047009y CCC: $27.50
Published on Web 09/15/2004

which were immerged in liquid nitrogen for cooling. This installation allows for a lowering of the sample temperature to 90 K, and for resistive heating to 1200 K. A K-type thermocouple was spot-welded to the edge of the crystal to monitor the temperature of the surface, and a homemade temperature controller was used to provide linear temperature ramps for the TPD experiments and to maintain the crystal to within ± 0.5 K of any specified temperature. The heating rate for all TPD measurements was set to 10 K/s. The Ni(110) crystal was cleaned before each experiment by repeated cycles of Ar^+ ion sputtering and annealing to 1100 K until the sample was deemed clean by XPS and the reported H_2 and CO TPD from the clean Ni(110) surface could be reproduced.[38]

Normal iodomethane (CH_3I, 99% purity) and fully deuterated iodomethane (CD_3I, 99.5% D) were purchased from Aldrich and used after several freeze−pump−thaw cleaning cycles. The H_2 (99.998% purity) and D_2 (99.5% D) gases were acquired from Matheson and used without further treatment. Exposure of the sample to all gases was accomplished by backfilling of the chamber using appropriate leak valves. The pressure was measured using a nude ion gauge, and the dosages were determined directly from the readings of the gauge (without calibration) and reported in units of langmuirs (1 langmuir $= 1 \times 10^{-6}$ Torr·s). All exposures were performed at constant surface temperatures: hydrogen and deuterium were dosed at 180 K, while iodomethane deposition was conducted at 90 K unless otherwise indicated.

Data acquisition for both XPS and TPD experiments was done by using an interfaced personal computer. Up to 15 masses could be followed in the TPD runs. The signal intensities were all calibrated to the same experimental parameters, and are reported in arbitrary units by the measuring bars in each of the figures. Most TPD spectra were deconvoluted using the cracking patterns of the appropriate molecules measured with our instrument.[25] A matrix $\mathbf{F}_{amu,comp}$ was first developed by measuring the intensities of the key ions in the cracking pattern (amu) of each one of the compounds to be deconvoluted (comp) using our mass spectrometer and experimental setup. Note was then taken of the fact that the partial pressures of those compounds, represented by a $\mathbf{P}_{comp}$ vector, is related to the mass spectroscopy intensities measured for each point in the TPD data, given by the vector $\mathbf{I}_{amu}$, by the matrix equation

$$\mathbf{I}_{amu} = \mathbf{F}_{amu,comp} \times \mathbf{P}_{comp} \quad (1)$$

Inversion of that equation allows for the direct estimation of the partial pressures of each compound from the raw TPD data according to the equation

$$\mathbf{P}_{comp} = \mathbf{F}_{amu,comp}^{-1} \times \mathbf{I}_{amu} \quad (2)$$

This conversion was computed using a spreadsheet for each of the TPD data sets for each temperature. An example of the starting raw data and the end result from this procedure is provided in Figure 1. Note that this procedure does potentially increase the noise level of the final TPD traces, in proportion to the number of compounds (amus) used in the deconvolution. Consequently, only the data for the compounds for which no unique mass with no significant interference from the other species could be found were processed this way.

To minimize the decomposition of the adsorbates induced by stray electrons, a grounded grid was set in front of the ion gauge and a negative bias was applied on the sample and holder. I 3d and C 1s XP spectra were averaged over a number of scans to obtain reasonable signal-to-noise ratios. The binding energies were calibrated against reported values using pure copper and gold samples as references.[40,41]

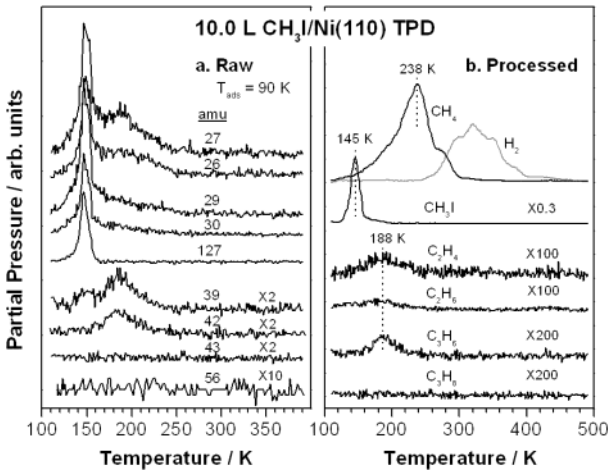

Figure 1. TPD spectra for 10.0 langmuirs of CH_3I dosed on a clean Ni(110) single-crystal surface at 90 K. The left panel shows the raw TPD traces for selected masses, while the right frame displays the corresponding deconvoluted spectra and provides information on the desorption of molecular iodomethane and all the other products detected, namely, hydrogen, methane, ethane, ethylene, and propylene. The production of the heavier alkanes and alkenes around 188 K appears to be unique to this crystallographic plane of nickel.

3. Results

3.1. Thermal Chemistry on Clean Ni(110). The thermal chemistry of iodomethane on Ni(110) surfaces was first characterized by TPD. Figure 1 shows typical TPD spectra for the case of a 10.0 langmuir CH_3I exposure at 90 K. The left panel reproduces the raw desorption traces, while the right frame displays the spectra for the different products after deconvolution of the raw data. The sharp peak around 145 K seen in several of the traces is due to molecular desorption of the iodomethane condensed in the multilayer. Additional desorption of ethylene and propene is seen at 188 K. A small amount of ethane is also seen at this temperature, but propane production is negligibly small. Methane desorption peaks at 238 K, and extends to 300 K. Finally, hydrogen from iodomethane decomposition is detected in several features between 250 and 380 K. Notice that the higher molecular weight hydrocarbons account for less than 0.3% of the iodomethane converted.

The dependence of the H_2, CH_4, and molecular TPD spectra for CH_3I on initial exposure is shown in Figure 2. Below 0.5 langmuir CH_3I doses no CH_4 desorbs at all, indicating that the adsorbates decompose completely to surface iodine, carbon, and hydrogen. Moreover, below 0.2 langmuir, the resulting atomic hydrogen recombines and desorbs in a single peak at 350 K, the same as for hydrogen adsorbed from the background gases (dotted line). Between 1.0 and 3.0 langmuirs, CH_4 desorption peaks at 274 K, but above those doses the major desorption intensity switches to a new feature at 238 K. Additional H_2 desorption peaks also develop in this CH_3I dose range, first at 321 K (starting at 0.5 langmuir), and then at 298 K (above 2.0 langmuirs). By a dose of 4.0 langmuirs, the leading edge of the methane desorption peak extends to temperatures below 150 K, and the three hydrogen peaks already seen at 3.0 langmuirs reach their final shape and intensities. Indeed, the desorption features for CH_4 and H_2 do not change significantly after exposures above 5.0 langmuirs.

The evolution of the molecular desorption with increasing coverage is reported in the right panel of Figure 2. These data

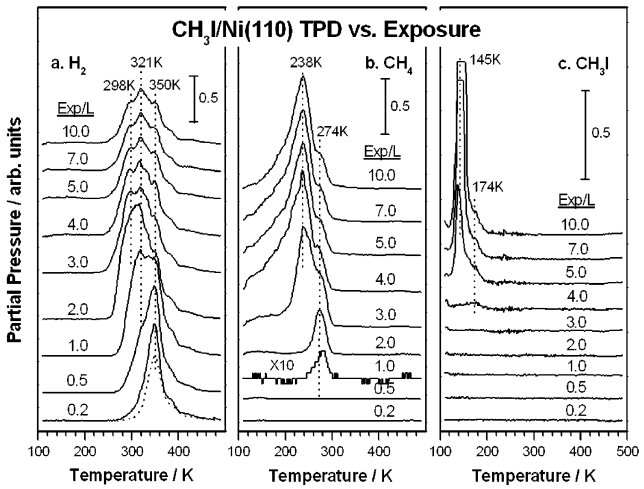

Figure 2. TPD spectra for (a) hydrogen (H_2), (b) methane (CH_4), and (c) molecular iodomethane (CH_3I) as a function of initial CH_3I exposure. The lowest spectrum (dotted line) in (a) represents the hydrogen trace due to background adsorption on the clean surface. Molecular desorption (c) was followed by the signal at 15 amu after deconvolution of the contribution from methane, and corroborated by the signals for the iodine (127 amu) and molecular (142 amu) ions. Only hydrogen is produced below 1.0 langmuir of CH_3I, in one peak around 350 K. Methane starts to desorb above 1.0 langmuir, initially at 274 K but mainly around 238 K for exposures above 3.0 langmuirs.

were acquired by following the signal for 15 amu (the CH_3^+ ion) after subtracting the contribution form methane fragmentation because of the better signal intensity compared to those of the other fragments in the CH_3I mass spectra, but the identity of the desorbing species was corroborated by the similar spectra obtained for 127 amu (Figure 1). Molecular desorption is only seen above 4.0 langmuirs, first as a small peak around 175 K from the first monolayer, and then in a sharp feature at 145 K due to multilayer condensation. Both the lack of changes in the H_2 and CH_4 TPD traces and the appearance of the 145 K peak for CH_3I between 4.0 and 5.0 langmuirs set this exposure as the onset for the growth of the second layer of the adsorbate.

The TPD yields for H_2, CH_4, and CH_3I as functions of CH_3I exposure are plotted in Figure 3. The H_2 TPD yield has been converted into monolayers using the coverage of hydrogen adsorbed from the background as reference, as reported before.[23] The CH_4 and CH_3I yields were then calibrated by using a mass balance argument and by assuming a saturation value for the CH_3I first layer of about 0.2 monolayers (ML).[23] Figure 3 shows that CH_4 production starts around 1.0 langmuir and increases up to 4.0 langmuirs but then levels off at a value of about 0.1 ML. The H_2 production, on the other hand, increases monotonically with CH_3I exposure up to a maximum of ~0.1 ML at 2.0 langmuirs and then decreases until reaching a value of about 0.05 ML above 5.0 langmuirs. It is interesting to note that the change in H_2 production above 2.0 langmuirs is stoichiometrically matched by the increase in CH_4 yield. This means that in effect the total decomposition of the adsorbed iodomethane increases up to 2.0 langmuirs and then levels off, and that the additional iodomethane adsorbed between exposures of 2.0 and 4.0 langmuirs is all hydrogenated to methane. Molecular desorption first appears between 4.0 and 5.0 langmuirs, and increases monotonically with increasing exposure afterward. The total CH_3I coverage, calculated via a weighted addition of the yields of the three main products (neglecting the production of heavier hydrocarbons), follows a linear behavior versus exposure up to monolayer saturation,[42] but then deviates slightly toward lower values, perhaps because of a blocking of some of the reacting sites by the molecules in the second layer.

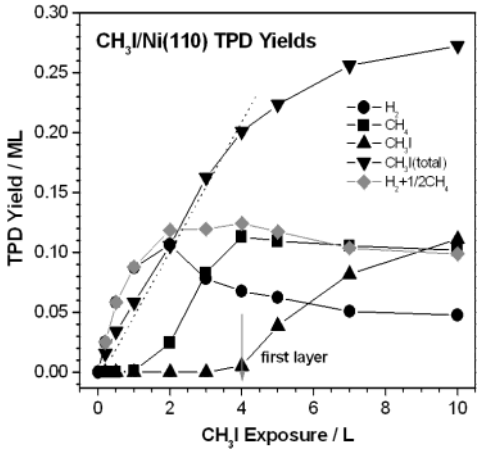

Figure 3. Coverage dependence of the TPD yields, in monolayers, for hydrogen, methane, and molecular desorption. Additional curves are provided for the total uptake of iodomethane (CH_3I(total)) and hydrogen ($H_2 + {}^1/_2CH_4$) in the monolayer, both calculated by using appropriate stoichiometric mass balance equations. Three regimes can be identified in this figure: below 2.0 langmuirs, where hydrogen desorption dominates, between 2.0 and 5.0 langmuirs, where significant methane is produced, and above 5.0 langmuirs, the exposure required for monolayer saturation, at which point molecular desorption starts.

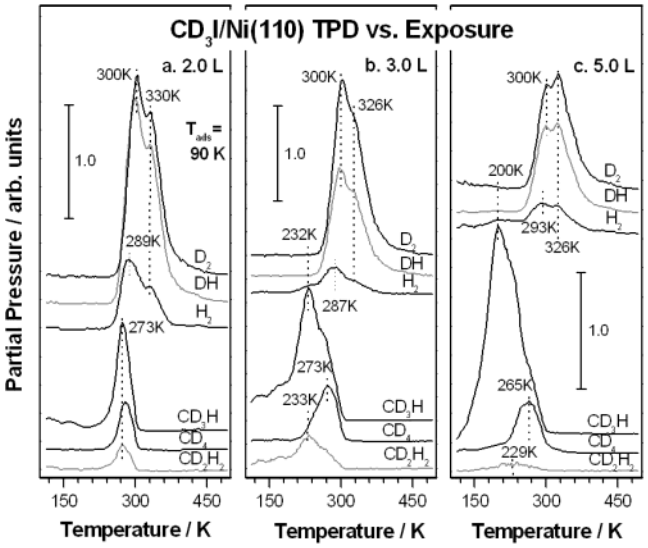

Figure 4. TPD spectra for three initial exposures, 2.0 (a), 3.0 (b), and 5.0 (c) langmuirs, of CD_3I on clean Ni(110). The methane spectra were deconvoluted using the cracking patterns of the different methane isotopologues. The similar shapes of the H_2, HD, and D_2 traces show complete isotope scrambling with normal hydrogen adsorbed from the background, and the production of significant quantities of CD_2H_2 indicates H−D exchange on the surface species. Also to note is the higher temperatures required to make perdeuteriomethane (CD_4) at high coverages.

3.2. Hydrogen Coadsorption. The production of methane on Ni(110) shown in Figure 2 differs from that on Ni(111)[23,43] and Ni(100)[22,26] in that it displays a complex TPD structure with at least two distinct peaks. The 274 K feature in particular develops below 2.0 langmuirs and remains as a shoulder in the high-temperature side of the desorption profile at higher coverages. To explore the origin of the two distinctive desorption features seen on this surface, additional TPD experiments were conducted with iodomethane-d_3. Figure 4 shows the TPD spectra obtained for H_2, HD, and D_2 and for CD_4, CD_3H, and CD_2H_2 after 2.0, 3.0, and 5.0 langmuir CD_3I exposures. (No significant CDH_3 or CH_4 production was observed, and therefore is not reported in the figure.) The desorption spectra of the different

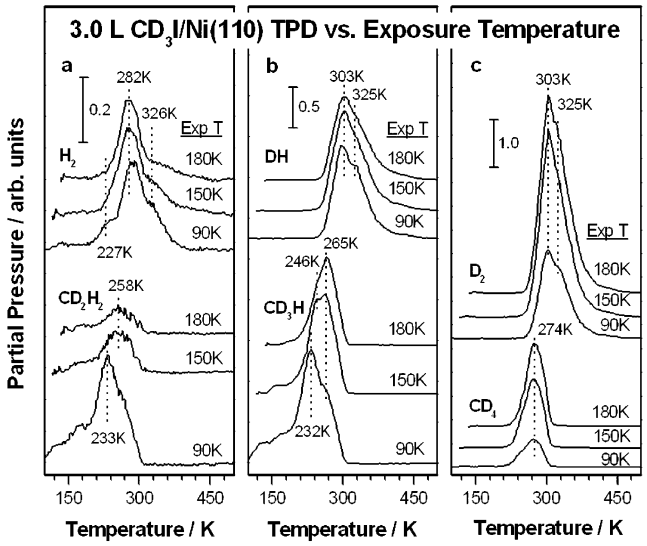

Figure 5. Influence of the deposition temperature on the thermal chemistry of 3.0 langmuirs of CD_3I on Ni(110). TPD for all relevant isotopologues of hydrogen and methane are reported for exposures at 90, 150, and 180 K. Increasing dosing temperatures minimize the time of exposure of the clean surface to the background gases, and therefore lower the coverage of the coadsorbed normal hydrogen on the surface. This is particularly manifested by the reductions in yields for CD_2H_2 and CD_3H.

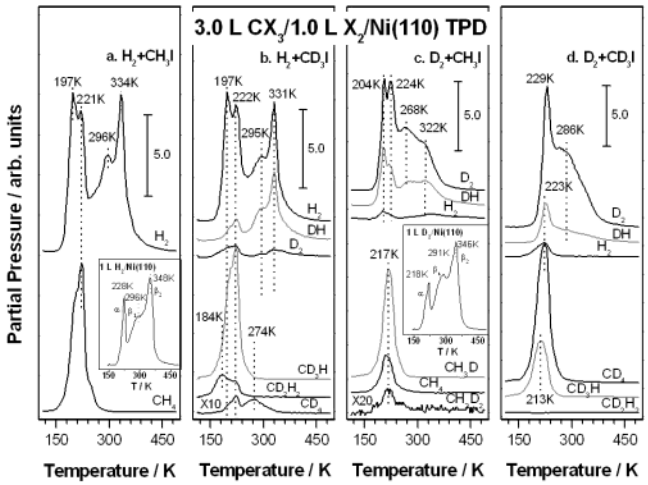

Figure 6. Hydrogen and methane TPD data for Ni(110) sequentially dosed with 1.0 langmuir of hydrogen (or deuterium) and 3.0 langmuirs of iodomethane (normal or perdeuterated). The results from all four isotope permutations are shown here, namely, $H_2 + CH_3I$ (a), $H_2 + CD_3I$ (b), $D_2 + CH_3I$ (c), and $D_2 + CD_3I$ (d). Complete isotope scrambling is seen in all the hydrogen desorption peaks, indicating some methyl dehydrogenation at temperatures as low as 150 K. All methane made by reductive elimination with coadsorbed hydrogen (deuterium) desorbs at low temperatures (~200 K), and only CD_4 from $H_2 + CD_3I$ is seen at 275 K.

methane isotopologues were obtained by deconvolution of the traces for 16−20 amu. The same as with normal iodomethane, an exposure of 2.0 langmuirs of CD_3I leads to the production of fully deuterated methane at temperatures around 274 K. In addition, the significant CD_3H and CD_2H_2 signals seen in that case demonstrate the high hydrogenation rate of the deuterated methyl intermediate by surface hydrogen from background adsorption as well as a degree of H−D exchange. When the surface is exposed to 3.0 langmuirs of CD_3I, the traces obtained for CD_3H and CD_2H_2 also show a similarity with that for CH_4 in the CH_3I(3 langmuirs)/Ni(110) case (Figure 2). On the other hand, CD_4 desorption still peaks at 273 K, even though it does extend slightly to lower temperatures. For the surface with 5.0 langmuirs of CD_3I, the CD_4 desorption peak broadens and shifts slightly to lower temperature, but still displays negligible intensity below 220 K, and only CD_3H is produced at those low temperatures. Also, the degree of H−D exchange indicated by the production of CD_2H_2 clearly decreases with increasing coverage, and the high-temperature shoulder in the CD_3H trace is less evident than that for CH_4 from CH_3I/Ni(110) (compare Figures 2 and 4).

Clearly, studies with CD_3I are complicated by the inevitable coadsorption of some normal hydrogen from the background. This undesirable coadsorption could be minimized by reducing the cooling time of the sample before CD_3I dosing, and by adsorbing the iodomethane at higher temperatures. Comparative experiments were carried out by dosing CD_3I at 90, 150, and 180 K (Figure 5). A clear increase in the production of the fully deuterated methane and a parallel decrease in CD_3H and CD_2H_2 yields are seen with increasing exposure temperatures. The effect of the deposition temperature for CD_3I is also reflected in the shape and position of the spectral structures for CD_2H_2 and CD_3H. On the other hand, the kinetics of the CD_4 desorption is only minimally influenced. Notice that, when CD_3I is dosed at 180 K, all methane isotopologues desorb in a single feature, yet the hydrogenation step to CD_3H still peaks at about 7 K lower temperatures than the reductive elimination to CD_4. A kinetic isotope effect is also seen in the hydrogen TPD spectra, with both HD and D_2 desorptions peaking at temperatures 20 K above those for H_2. For the case of CD_3I exposure at 150 K, a low-temperature shoulder appears in the CD_3H trace at 246 K, indicating more hydrogen coadsorption from the background, and dosing at 90 K leads to TPD traces for both CD_2H_2 and CD_3H with the same features seen in CH_3I(3 langmuirs)/Ni-(110).

The effect of predosing either hydrogen or deuterium on the conversion of the methyl species on Ni(110) was examined by using both CH_3I and CD_3I precursors (Figure 6). In these experiments, 1.0 langmuir of hydrogen or deuterium was dosed first, after which 3.0 langmuirs of iodomethane was adsorbed. In the coadsorption systems with normal hydrogen, the H_2 TPD spectra reproduce well those obtained for hydrogen dosed alone on clean Ni(110), with their three desorption states labeled α, β_1, and β_2 (Figure 6a, inset),[44] but also show an additional sharp feature at 197 K. The D_2 TPD spectra in the coadsorbed system, however, display significant changes relative to the TPD for deuterium adsorbed alone (Figure 6c, inset), especially in the population of the β_2-state. We are not clear on what the reason for this difference may be, except a possible change in the final surface hydrogen vs deuterium coverages. In terms of methane production, CH_4 desorption from CH_3I(3 langmuirs)/H_2(1 langmuir)/Ni(110) differs from that from CH_3I/Ni(110) (Figure 2) in that there is a ~20 K downward shift in the overall spectrum. In addition, the high-temperature shoulder seen on clean Ni-(110) is almost gone. Similar behavior was observed in the CH_3I(3 langmuirs)/D_2(1 langmuir)/Ni(110) and CD_3I(3 langmuirs)/D_2(1 langmuir)/Ni(110) systems reported in this figure, except for the additional complications arising from possible kinetic isotope effects. The CD_2H_2 traces in both parts b and c of Figure 6 indicate that the isotope scrambling is initiated at temperatures as low as 150 K, but it is interesting to note that in the CD_3I(3 langmuir)/H_2(1 langmuir)/Ni(110) combination the fully deuterated methane displays distinctive peaks at 274 and 220 K similar to those seen with CH_3I/Ni(110) at the same exposure (Figure 2). In general, desorption of all H_2, HD, and D_2 is seen with CD_3I and/or D_2, except that most of the hydrogen

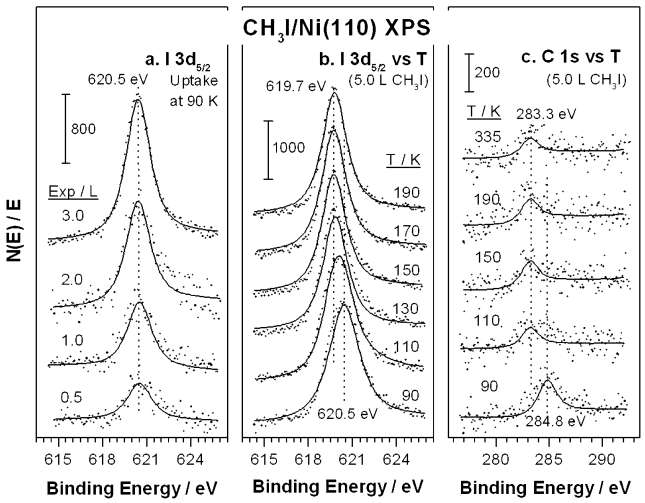

Figure 7. I $3d_{5/2}$ (a, b) and C 1s (c) XP spectra evidencing the C−I bond scission that results from thermal activation of CH_3I adsorbed on Ni(110). The left panel (a) provides the I $3d_{5/2}$ XPS for the CH_3I uptake at 90 K, indicating molecular adsorption regardless of coverage. The other two panels, which provide the I $3d_{5/2}$ (b) and C 1s (c) XPS annealing sequences for an initial 5.0 langmuir CH_3I exposure, show shifts from 110 to 150 K associated with the conversion of adsorbed iodomethane to methyl and iodine surface species.

(or deuterium) originating from the iodomethane desorbs at the higher temperatures. This is especially evident in Figure 6b. Also, in the methane TPD spectra from CD_3I(3 langmuirs)/H_2-(1 langmuir)/Ni(110) the fully deuterated isotopologue accounts for only 2% of the total methane production, but with CD_3I(3 langmuirs)/D_2(1 langmuir)/Ni(110) and CD_3I(3 langmuirs)/Ni-(110) the CD_4 yields amount to 70% and 21%, respectively.

3.3. XPS Data. Both the scission of the C−I bond in adsorbed iodomethane that leads to the formation of surface methyl groups and the nature of the resulting hydrocarbon moieties were characterized by XPS. The key data obtained from these experiments are shown in Figure 7. The first panel shows the I $3d_{5/2}$ signal in uptake experiments at 90 K. One single peak is seen at all coverages centered at 620.5 eV, the same value within experimental error reported for other iodohydrocarbons on nickel surfaces.[25,37,45] On the other hand, the annealing sequence in the middle panel, which corresponds to a 5.0 langmuir CH_3I exposure, shows a shift in binding energy to 619.7 eV starting around 110 K and finishing by 150 K, indicative of the scission of the C−I bond in the adsorbed molecules.[25,26]

The C 1s XP spectra shown in Figure 7c, although quite noisy, corroborates the observation of the C−I bond activation implied by the I $3d_{5/2}$ spectra. In particular, the initial 284.8 eV peak at 90 K and the final 283.3 eV peak above 150 K represent the two different chemical states of carbon in the CH_3I_{ads} and $CH_{x,ads}$ species, respectively. That conversion starts around 110 K and reaches completion by 150 K, the same temperature range reported for the changes in the I $3d_{5/2}$ signal. The variations in the C 1s XPS intensities with increasing annealing temperatures of the sample can also be used to estimate the extent of the iodomethane to methyl surface conversion. First, an absolute signal calibration was obtained by using the TPD data in Figure 3, where a 5.0 langmuir CH_3I exposure on the Ni(110) surface at 90 K was estimated to correspond to a 0.225 ML coverage. It is then seen from the C 1s XPS data that heating to 150 K leads to a 75% conversion of the CH_3I precursor into $CH_{x,ads}$; the remaining 25% desorbs from the surface, either molecularly and/or in the form of CH_4. Further reduction of the C 1s XPS peak is observed upon continuing heating because of additional CH_4 desorption. Even though no chemical shifts with respect to the C_1 hydrocarbons could be identified in the C 1s XPS data, the residual carbon detected after annealing at 335 K, which amounts to ∼40% of the initial value, can be assumed to be in the form of the atomic carbon that forms after total decomposition.

4. Discussion

Continuing with our studies on the chemistry of C_1 hydrocarbon fragments on metal surfaces, here CH_3I was used as a precursor to produce and characterize the chemistry of CH_3 species on a Ni(110) surface. As in other similar systems, it was found that CH_3I dosed at 90 K adsorbs molecularly.[12,13,23,46−51] On the other hand, according to both I $3d_{5/2}$ and C 1s XP spectra, the majority of the C−I bonds of the CH_3I adsorbed precursors break below 130 K, although some molecular desorption takes place around 145 K (Figure 1). For CH_3I exposures below 5.0 langmuirs, which corresponds to monolayer saturation, the subsequent thermal chemistry of the surface methyl intermediates produced by this C−I bond scission is dominated by dehydrogenation and hydrogenation steps leading to hydrogen and methane desorption, respectively. That chemistry appears to follow complex kinetics depending on the initial coverage of the iodide. For doses below 2.0 langmuirs of CH_3I, single peaks are seen in the TPD traces for H_2 and CH_4, around 350 and 275 K, respectively. Also, total decomposition dominates at those coverages; no methane production at all is seen below 1.0 langmuir, and only about 25% of the initial iodomethane is converted to CH_4 after a 2.0 langmuir dose. On the other hand, between 3.0 and 5.0 langmuir CH_3I exposures, three peaks are seen in the H_2 TPD traces at 298, 321, and 350 K, and methane is mostly produced at about 238 K. By 5.0 langmuirs, methane desorption accounts for about 75% of all the adsorbed iodomethane, and the H_2 yield amounts to only half of the maximum seen for 2.0 langmuirs.

The chemistry of CH_3I on Ni(110) in the intermediate 2.0−5.0 langmuir coverage range is certainly more complex than that previously reported on the Ni(100)[19,26] and Ni(111)[23,43] surfaces, where only one CH_4 TPD peak is observed. It is clear from the TPD data for iodomethane with coadsorbed hydrogen (or deuterium) in Figure 6 that methane formation is possible around 220 K as long as there is atomic hydrogen (deuterium) on the surface. The implication is that on the clean nickel the rate-limiting step for that reaction is the decomposition of some of the surface methyl groups needed to generate the required hydrogen. Moreover, the CD_4 TPD traces for both pure CD_3I (Figure 4) and H_2 + CD_3I (Figure 6b) show that the perdeuteriomethane can only be produced around 270 K. That indicates no dedeuteriation (C−D dissociation) below approximately 230 K, the onset of the CD_4 peak. However, the majority of the methane produced after CH_3I exposures above 3.0 langmuirs desorbs in the 238 K peak, which displays a long leading edge extending all the way to 100 K (Figure 2). This low-temperature methane desorption cannot be accounted for by incorporation of hydrogen from the background alone, and must therefore imply some limited methyl surface decomposition at high coverages. In addition, early methyl dehydrogenation is implicated in the H−D exchange evident in Figures 4 and 5a by the appearance of a sizable TPD peak for CD_2H_2. Complete isotope scrambling is also seen in all hydrogen TPD peaks (Figures 4−6): note in particular the desorption of some deuterium in the 197 K peak with H_2 + CD_3I in Figure 6b. The somewhat contradictory results seen with CH_3I vs CD_3I may be explained by a normal kinetic isotope effect, which makes perdeuteriom-

ethyl surface species somewhat more stable than their normal $CH_{3,ads}$ counterparts. In any case, it can be argued that dehydrogenation of methyl groups on Ni(110) surfaces starts below 150 K. It also appears that dehydrogenation is limited, and results in the buildup of a significant population of methylene groups on the surface.

The other main difference in the chemistry of iodomethane on Ni(110) versus Ni(100) or Ni(111) is that at exposures above 5.0 langmuirs heavier hydrocarbons, specifically ethylene, ethane, and propene, are produced. However, it is worth pointing out that the yields for these only amount to 0.3% or less of the total hydrocarbon production (Figure 1). In the case of CH_2I_2, those hydrocarbons are produced at exposures as low as 3.0 langmuirs, and account for approximately 10% of the total hydrocarbon production.[25] This comparison indicates that methylene intermediates are critical for the carbon−carbon chain growth, and control the final yields of heavier hydrocarbons. The initial step is likely to be a migratory insertion of methylene into a nickel−methyl bond to form an ethyl surface intermediate. Subsequent β-hydride elimination from that ethyl accounts for the production of ethylene, while reductive elimination with surface hydrogen explains the formation of ethane. Assuming that ethyl formation is rate-limiting explains the similar kinetics observed for the alkane and olefin production, and a second methylene insertion followed by an analogous β-hydride elimination from the resulting propyl intermediates the desorption of propene. This mechanism was shown operative with surface methylene groups by using selective isotope labeling.[25]

More alkenes than alkanes are produced in this iodomethane/Ni(110) system. This may be due either to a faster rate of β-hydride elimination compared to that of reductive elimination with H atoms, and/or to a limited supply of surface hydrogen. As a consequence, the observed ethylene-to-ethane yield ratio amounts to approximately 3:1, and the production of propane is negligibly small. Independent experiments with iodoethane, a precursor for surface ethyl groups, corroborate this conclusion: there, ethylene and ethane are produced at 190 and 205 K, respectively, in a ~5:1 yield ratio.[52] Also, the depletion of the methylene intermediates on the surface makes the probability for the third insertion step quite small, thus the lack of any detectable butene production in our TPD experiments. Alternatively, ethane production could potentially originate from direct coupling of two CH_3 surface groups, but this is unlikely because of the similar kinetics and higher yield for C_2H_4 production. As it is much easier to hydrogenate a small amount of $CH_{2,ads}$ to $CH_{3,ads}$ than to build up large concentrations of surface $CH_{2,ads}$ from $CH_{3,ads}$, a smaller $CH_{2,ads}$ population is obtained when starting with CH_3I, and that explains the lesser extent of the chain growth reported here when compared to the experiments with CH_2I_2.

5. Conclusions

Both I $3d_{5/2}$ and C 1s XP spectra evidenced that the scission of the C−I bond in CH_3I adsorbed on Ni(110) proceeds at temperatures between 110 and 150 K regardless of surface coverage. Isotope-labeling experiments corroborated that dehydrogenation of some of the resulting methyl intermediates starts around 150 K, but it is limited, especially at high coverages, and produces methylene surface intermediates. Both hydrogenation of methyl groups to methane and H−D exchange via a fast methyl−methylene surface interconversion occur with complex kinetics affected by the initial coverages of the iodomethane and any coadsorbed hydrogen or deuterium. A small amount of heavier hydrocarbons, alkenes and alkanes, are also produced via a rate-limiting methylene migratory insertion step to ethyl moieties followed by facile β-hydride elimination and reductive elimination with surface hydrogen. However, this chemistry takes place with much less efficiency than when starting with methylene surface groups, presumably because of the relatively low concentration of those groups therefore produced by methyl dehydrogenation.

Acknowledgment. Financial support for this work was provided by the U.S. National Science Foundation.

References and Notes

(1) Biloen, P.; Sachtler, W. M. H. *Adv. Catal.* **1981**, *30*, 165.
(2) Dry, M. E. *Catal. Today* **2002**, *71*, 227.
(3) Vannice, M. A. *Catal. Rev.—Sci. Eng.* **1976**, *14*, 153.
(4) Choudhary, T. V.; Aksoylu, E.; Goodman, D. W. *Catal. Rev.—Sci. Technol.* **2003**, *45*, 151.
(5) Zaera, F. *J. Phys. Chem. B* **2002**, *106*, 4043.
(6) Somorjai, G. A. *Introduction to Surface Chemistry and Catalysis*; John Wiley & Sons: New York, 1994.
(7) Zaera, F. *Catal. Lett.* **2003**, *91*, 1.
(8) Zaera, F. *Chem. Rev.* **1995**, *95*, 2651.
(9) Bent, B. E. *Chem. Rev.* **1996**, *96*, 1361.
(10) Queeney, K. T.; Chen, D. A.; Friend, C. M. *J. Am. Chem. Soc.* **1997**, *119*, 6945.
(11) White, J. M. *J. Mol. Catal. A* **1998**, *131*, 71.
(12) Solymosi, F. *Catal. Today* **1996**, *28*, 193.
(13) Zhou, X. L.; Solymosi, F.; Blass, P. M.; Cannon, K. C.; White, J. M. *Surf. Sci.* **1989**, *219*, 294.
(14) Paul, A. M.; Bent, B. E. *J. Catal.* **1994**, *147*, 264.
(15) Chiang, C. M.; Wentzlaff, T. H.; Jenks, C. J.; Bent, B. E. *J. Vac. Sci. Technol., A* **1992**, *10*, 2185.
(16) Lin, J.-L.; Bent, B. E. *J. Phys. Chem.* **1993**, *97*, 9713.
(17) Lin, J. L.; Chiang, C. M.; Jenks, C. J.; Yang, M. X.; Wentzlaff, T. H.; Bent, B. E. *J. Catal.* **1994**, *147*, 250.
(18) Jenks, C. J.; Bent, B. E.; Zaera, F. *J. Phys. Chem. B* **2000**, *104*, 3017.
(19) Tjandra, S.; Zaera, F. *Langmuir* **1992**, *8*, 2090.
(20) Tjandra, S.; Zaera, F. *J. Am. Chem. Soc.* **1992**, *114*, 10645.
(21) Tjandra, S.; Zaera, F. *J. Catal.* **1993**, *144*, 361.
(22) Tjandra, S.; Zaera, F. *Langmuir* **1993**, *9*, 880.
(23) Tjandra, S.; Zaera, F. *J. Catal.* **1994**, *147*, 598.
(24) Azizian, S.; Gobal, F. *J. Mol. Catal. A* **2000**, *153*, 191.
(25) Guo, H.; Zaera, F. *Surf. Sci.* **2003**, *547*, 284.
(26) Zhou, X. L.; White, J. M. *Chem. Phys. Lett.* **1987**, *142*, 376.
(27) Zaera, F. *Acc. Chem. Res.* **1992**, *25*, 260.
(28) Zaera, F. *Prog. Surf. Sci.* **2001**, *69*, 1.
(29) Zaera, F. *J. Mol. Catal.* **1994**, *86*, 221.
(30) Janssens, T. V. W.; Zaera, F. *J. Catal.* **2002**, *208*, 345.
(31) Weldon, M. K.; Friend, C. M. *Chem. Rev.* **1996**, *96*, 1391.
(32) Solymosi, F. *J. Mol. Catal. A* **1998**, *131*, 121.
(33) Tjandra, S.; Zaera, F. *J. Vac. Sci. Technol., A* **1992**, *10*, 404.
(34) Lin, J.-L.; Teplyakov, A. V.; Bent, B. E. *J. Phys. Chem.* **1996**, *100*, 10721.
(35) Zaera, F. *Surf. Sci.* **1989**, *219*, 453.
(36) Zaera, F.; Hoffmann, H. *J. Phys. Chem.* **1991**, *95*, 6297.
(37) Tjandra, S.; Zaera, F. *J. Am. Chem. Soc.* **1995**, *117*, 9749.
(38) Chrysostomou, D.; Flowers, J.; Zaera, F. *Surf. Sci.* **1999**, *439*, 34.
(39) Guo, H.; Chrysostomou, D.; Flowers, J.; Zaera, F. *J. Phys. Chem. B* **2003**, *107*, 502.
(40) *Handbook of X-Ray Photoelectron Spectroscopy*; Wagner, C. D., Riggs, W. M., Davis, L. E., Moulder, J. F., Muilenberg, G. E., Eds.; Perkin-Elmer Corp.: Eden Prairie, MN, 1978.
(41) Guo, H.; Zaera, F. *Catal. Lett.* **2003**, *88*, 95.
(42) Zaera, F.; Tjandra, S. *J. Phys. Chem.* **1994**, *98*, 3044.
(43) Castro, M. E.; Chen, J. G.; Hall, R. B.; Mims, C. A. *J. Phys. Chem. B* **1997**, *101*, 4060.
(44) Winkler, A.; Rendulic, K. D. *Surf. Sci.* **1982**, *118*, 19.
(45) Zhao, Q.; Zaera, F. *J. Phys. Chem. B* **2003**, *107*, 9047.
(46) Zhou, Y.; Henderson, M. A.; Feng, W. M.; White, J. M. *Surf. Sci.* **1989**, *224*, 386.
(47) Zaera, F. *Surf. Sci.* **1992**, *262*, 335.
(48) Lin, J.-L.; Bent, B. E. *J. Vac. Sci. Technol., A* **1992**, *10*, 2202.
(49) Solymosi, F.; Revesz, K. *Surf. Sci.* **1993**, *280*, 38.
(50) Bugyi, L.; Oszko, A.; Solymosi, F. *J. Catal.* **1996**, *159*, 305.
(51) Wu, G.; Kaltchev, M.; Tysoe, W. T. *Surf. Rev. Lett.* **1999**, *6*, 13.
(52) Guo, H.; Zaera, F. To be published.